# Determination of the crystallized fractions of a largely amorphous multiphase material by the Rietveld method

**X. Orlhac,[a]\* C. Fillet,[a] P. Deniard,[b] A. M. Dulac[b] and R. Brec[b]**

[a]Commissariat à l'Energie Atomique, Valrhô-Marcoule, DRRV/SCD, BP 171, 30207 Bagnols-sur-Cèze CEDEX, France, and [b]Institut des Matériaux de Nantes, Laboratoire de Chimie du Solide, 44322 Nantes CEDEX 3, France. Correspondence e-mail: xavier.orlhac@saint-gobain.com

The Rietveld method has proved to be a very effective means to characterize and quantify the crystalline phases and the amorphous phase in glass ceramic materials using X-ray powder diffraction data. The technique was applied to a borosilicate glass of the type used for high-level nuclear-waste containment, in order to measure the proportions of the crystallized phases after heat treatment and, thus, to qualify the thermal stability of the glass. Six crystalline phases were analysed in this way in an almost entirely (>95 wt%) amorphous material after adding a known proportion of an internal standard ($TiO_2$). The quantitative analyses were corrected to allow for microabsorption effects resulting from grain-size and absorption-contrast effects. In addition to the quantitative data, unit-cell parameters and site-occupancy refinements revealed solid-solution and substitution phenomena in the crystal.

## 1. Introduction

The use of vitreous materials for the containment of high-level nuclear waste requires knowledge of their long-term behaviour and, notably, of the nature and extent of possible devitrification. Crystallization is undesirable for the confinement of a fission product solution as it is liable to affect the properties of the containment glass: homogeneity, incorporation of radionuclides into the glass structure, stability and chemical durability.

A devitrification study was performed on a nonradioactive glass comparable to the French nuclear glass in order to assess its thermal stability and to determine its devitrification capacity. The glass was heated to temperatures at which the kinetics are fast enough to obtain material changes within measurable time frames. The objective of this study was to quantify the fractions of the crystalline phases that appeared in the glass after heat treatment. The crystalline phases were identified by X-ray diffraction on powder specimens. The mass fractions of each phase were determined by applying the Rietveld method, adapted here to analyse largely amorphous polyphase materials. Corrections were applied to allow for microabsorption effects. Results are compared with other experimental data obtained by chemical and optical micrography analysis.

## 2. Description of the method

The Rietveld quantitative analysis method is based on the fact that the intensity diffracted by a crystalline phase is proportional (with suitable corrections) to the quantity of diffracting material (Rietveld, 1969; Bish & Howard, 1988). The principle involves theoretically reconstituting the complete diffraction profile by gradually refining the unit-cell and structural parameters. Other parameters are introduced to take into account line widths, or to compensate for the effects of preferred orientation, angular shifts, atomic displacement parameters (Debye–Waller factors), *etc.*

Refinement consists of determining, through the method of least squares, the model parameter values that provide the best agreement between observed and calculated diagrams. Among the refinement parameters, the scale factor $S$ accounts for the intensity diffracted by each crystalline phase. This parameter alone expresses the quantity of phase $\varphi$ in the sample (Bish & Howard, 1988):

$$S_\varphi = (C/\bar{\mu})\,[W_\varphi/(ZMV)_\varphi], \qquad (1)$$

where $W_\varphi$ is the weight fraction of phase $\varphi$ with a molecular weight $M_\varphi$, $Z_\varphi$ is the number of molecules in a cell of unit volume $V_\varphi$, $\bar{\mu}$ is the mean absorption coefficient of the mixture (weighted by the linear absorption coefficients of each phase) and $C$ is an experimental constant. Assuming that the multiphase sample is fully crystallized, the sum of the weight fractions can be constrained to 1 in order to calculate the relative weight fraction of each phase $\varphi$:

$$W_\varphi = S_\varphi(ZMV)_\varphi \Big/ \sum_{i=1}^{n} S_i(ZMV)_i. \qquad (2)$$

When a mixture contains an amorphous phase, the weight fractions of each phase $\varphi$ in the sample can be determined by introducing a known proportion of an internal standard ($W_{std}$). Thus, $(W_\varphi)_x$ is the weight fraction observed by X-ray

diffraction, $(W_\varphi)_{real}$ is the weight fraction in the powder containing the standard, and $(W_\varphi)_{raw}$ is the weight fraction in the sample.

The weight fractions observed by X-ray diffraction, $(W_\varphi)_x$, must be corrected to allow for the presence of the amorphous phase by applying the following relation:

$$(W_\varphi)_{real} = (W_\varphi)_x (W_s)_{real}/(W_s)_x. \qquad (3)$$

Another correction is required to subtract the contribution of the standard and thus to obtain the weight fraction of phase $\varphi$, $(W_\varphi)_{raw}$, actually present in the sample:

$$(W_\varphi)_{raw} = (W_\varphi)_{real}/[1 - (W_s)_{real}]. \qquad (4)$$

The above calculated phase percentages do not take into account microabsorption effects. The powder grain size and surface roughness result in a systematic microabsorption error, notably in the case of coarse powders containing mixture components with very different linear absorption coefficients. Brindley (1945) defined the 'mean powders' by the following relation:

$$0.01 < 2r\mu_\varphi < 0.1, \qquad (5)$$

where $r$ is the mean crystallite radius and $\mu_\varphi$ is the linear absorption coefficient of phase $\varphi$ determined from the weighted mean atomic absorption coefficients:

$$\mu_\varphi = (N/V) \sum_{i=1}^{n} \mu_{a_i}, \qquad (6)$$

in which $N$ is the number of patterns per cell and $\mu_{a_i}$ is the atomic absorption coefficient of element $i$ in the cell. $\mu_{a_i}$ is given in the *International Tables for Crystallography* (1983) for a monocrystal and must be multiplied by the packing density in the case of powder samples.

When the compound consists of 'mean powders' as defined by Brindley, equation (2) is modified to take account of the absorption contrast factor $\tau_\varphi$ (Brindley coefficient) of phase $\varphi$:

$$W_\varphi = \frac{S_\varphi (ZMV)_\varphi/\tau_\varphi}{\left[\sum_{i=1}^{n} S_i (ZMV)_i\right]/\tau_i}. \qquad (7)$$

For low absorption-contrast values, *i.e.* $-0.1 \leq (\mu_\varphi - \bar{\mu})r \leq 0.1$, the $\tau_\varphi$ values are given empirically by the following polynomial expression:

$$\tau_\varphi = 1 - 1.450(\mu_\varphi - \bar{\mu})r + 1.426[(\mu_\varphi - \bar{\mu})r]^2. \qquad (8)$$

The $\tau_\varphi$ coefficients are first calculated from equation (8) using the weight fractions given by the Rietveld refinement. They are then substituted in equation (7) to correct the weight fractions. This procedure is reiterated until the Brindley coefficients converge.

## 3. Experimental procedure

### 3.1. Specimen fabrication and preparation

The tests were carried out with a borosilicate glass (refer to weight composition in Table 1) prepared in a stirred platinum crucible at 1473 K and poured onto a plate to prevent devi-

**Table 1**
Glass composition (wt%).

| | | | |
|---|---|---|---|
| SiO$_2$ | 45.12 | ZrO$_2$ | 2.71 |
| B$_2$O$_3$ | 13.92 | MoO$_3$ | 1.75 |
| Na$_2$O | 10.06 | Cs$_2$O | 1.10 |
| Al$_2$O$_3$ | 4.92 | BaO | 0.61 |
| CaO | 4.01 | TeO$_2$ | 0.23 |
| Li$_2$O | 1.96 | La$_2$O$_3$ | 0.92 |
| ZnO | 2.49 | Ce$_2$O$_3$ | 0.95 |
| Fe$_2$O$_3$ | 2.98 | Nd$_2$O$_3$ | 1.63 |
| NiO | 0.42 | Pr$_2$O$_3$ | 0.45 |
| Cr$_2$O$_3$ | 0.52 | Y$_2$O$_3$ | 0.20 |
| P$_2$O$_5$ | 0.29 | RuO$_2$ | 1.52 |
| SrO | 0.34 | Pd | 1.20 |

trification during cooling. Two platinoid elements remained unmelted at the glass-processing temperature: a polymetallic Pd–Te phase consisting of spherical particles ranging from 1 to 25 µm in radius, and ruthenium oxide RuO$_2$ in the form of micrometric rodlets. The platinoid elements were present from the outset and were unaffected by heat treatment, but they did favour the crystallization of new phases (Orlhac *et al.*, 1998).

The glass fragments were first crushed to a fine powder in an agate mortar, then crushed again with TiO$_2$ (anatase) as an internal standard (selected to ensure minimum overlapping between its diffraction peaks and those of the sample itself); 8 wt% TiO$_2$ was added to obtain intensity values comparable to those of the crystalline phases. The powder was placed on a plate with a circular recess and scraped flush with the surface using a ground glass slide to avoid any preferred grain orientation. The plate was then positioned so that the sample surface was perfectly flat and tangential to the goniometer focusing circle.

Four samples were analyzed in this study: a quenched glass powder, containing only insoluble (platinoid) elements, and three samples of the same glass powder heat-treated for 20, 50 and 1000 h at 1023 K.

### 3.2. Experimental conditions

The diffraction data were obtained at room temperature using a Bragg–Brentano diffractometer (Siemens D5000) in $\theta/\theta$ geometry, with a Cu anticathode (40 kV, 30 mA) and a linear detector. The 10–100° ($2\theta$) angular range was scanned in 0.03° ($2\theta$) steps. In view of the very small crystallized-phase percentages in the powder samples, the counting time was set at 17 s step$^{-1}$.

### 3.3. Rietveld refinement

After identifying the crystalline phases present in the sample, the weight percentages of all the detected phases were calculated by applying Rietveld refinement in three steps using the *FullProf* software (Rodriguez-Carvajal, 1993).

(i) As the material was mainly amorphous, the significant continuous background was refined using a sixth-order polynomial or by interpolation of some chosen background points.

(ii) The line profile was initially analysed by whole-pattern fitting with no structural constraint, to refine the sample offset,

**Table 2**
Structural and thermal data concerning the appearance of the identified crystalline phases.

| Crystalline phase | Temperature range of appearance (K) (Orlhac et al., 1998) | Identification (JCPDS) | Space group | Unit-cell parameters (a, b, c) |
|---|---|---|---|---|
| $RuO_2$ | Glass heterogeneity | 43-1027 | $P4_2/mnm$ | (4.492, 4.492, 3.107) |
| Pd–Te | Glass heterogeneity | 05-0681 | $Fm3m$ | (3.896, 3.896, 3.896) |
| $CaMoO_4$ | 903–1153 | 29-0351 | $I4_1/a$ | (5.226, 5.226, 11.430) |
| $CeO_2$ | 1023–1173 | 34-0394 | $Fm3m$ | (5.411, 5.411, 5.411) |
| $ZnCr_2O_4$ | 1023–1473 | 22-1107 | $Fd3m$ | (8.328, 8.328, 8.328) |
| $TiO_2$ | Internal standard | 21-1272 | $I4_1/amd$ | (3.785, 3.785, 9.516) |

the unit-cell parameters, the profile evolution and the full width at half-maximum *versus* the diffraction angle.

(iii) Rietveld refinement ultimately made it possible to refine the scale factors, atomic positions, site occupancies and atomic displacement parameters (Debye–Waller).

## 4. Results and discussion

### 4.1. Identification of crystalline phases

Analysis of the quenched-glass diffraction diagram reveals the presence of the internal standard ($TiO_2$) and of the expected platinoid elements: ruthenium oxide ($RuO_2$) and the Pd–Te solid solution. Three additional phases appear on the heat-treated glass diffraction diagrams (Fig. 1): calcium molybdate ($CaMoO_4$), cerium oxide ($CeO_2$) and spinel ($ZnCr_2O_4$). The structural data for all the phases observed are indicated in Table 2, together with the temperature range in which they appeared.

### 4.2. Refinement of the powder X-ray diffraction diagrams

All glass samples were quantitatively analysed using the Rietveld method. In each case, the quality of the refinement was confirmed by the reliability factors and by visual examination of the plotted difference between the measured and calculated profiles (Fig. 2).

No major variations in the unit-cell parameters for the stoichiometric phases in the studied glass samples were noted after refinement. However, in the case of the Pd–Te solid solution, the initial refinement based on the cubic lattice of palladium resulted in a significantly higher unit-cell parameter compared with pure palladium: *a* increased from 3.896 to 3.915 Å. Based on Chattopadhyay's study of Pd–Te unit-cell parameter variations as a function of the composition (Chattopadhyay *et al.*, 1986), the solid-solution composition was determined to be Pd–5Te (at.%). This finding was confirmed by electron microprobe analysis [Pd–4.5Te (at.%)], thus demonstrating that the Rietveld method provides data on the content of the crystal structure through variations in the unit-cell parameters.

### 4.3. Correction applying the Brindley method

The results of the Rietveld-based quantitative analysis of crystalline phases were corrected by the Brindley method to take into account microabsorption phenomena. The $\tau_\varphi$ coefficients were first estimated from the empirical relation (8) using the linear absorption coefficients $\mu_\varphi$ calculated from equation (6) with a powder compactness factor of 0.35. This value was estimated from the comparison between measured and calculated absorption coefficients of different known materials used in the same data collection geometry. A mean crystallite radius of 10 μm was assumed for all the phases observed, based on a microscopic analysis of the samples (despite the wide scattering of the Pd–Te solid-solution size range). In order to calculate $\bar{\mu}$ (the weighted sum of the $\mu_\varphi$ coefficients, including the amorphous phase), it was first necessary to determine the linear absorption coefficient of the amorphous phase. This was impossible from a theoretical standpoint, considering the complexity of the initial glass, and was therefore obtained experimentally, through a powder diffraction experiment, by absorption in a known thickness of glass. The powder was placed between two beryllium windows in an Inel CPS 120 diffractometer in Debye–Scherrer geometry. The linear absorption of the amorphous phase was determined from the Beer–Lambert equation:

$$I = I_0 \exp(-\mu e), \tag{9}$$

where *e* is the powder thickness, and *I* and $I_0$ are the intensities of the transmitted and incident beams, respectively. The relatively low value obtained ($\mu = 110 \text{ cm}^{-1}$) reflects the predominance of light elements in the glass composition.

Having thus determined the linear absorption coefficients for all the phases, it was then possible to correct the phase percentage values to allow for microabsorption. The results of Rietveld refinement, corrected for the presence of the internal standard, and before and after correction for microabsorption, for glasses quenched and heat-treated for 20, 50 and 1000 h at 1023 K, are presented in Table 3. Note that correcting for microabsorption resulted in an increase in the crystallized weight fractions for the heat-treated glass. This effect is particularly observed for highly absorbing material, which is largely underestimated by the quantitative analysis. The amorphous-phase weight fraction was calculated by subtracting the sum of the crystallized-phase weight percentages.

Recent studies have demonstrated the ability of the Rietveld method to quantify synthetic mixtures with less than ±3% error (Yasukawa *et al.*, 1998). The error on the calculated crystallized fractions results primarily from the estimated standard deviation of the scale factor, $S_\varphi$, determined in the least-squares refinement. The error on the weight of the internal standard is assumed to be negligible. The errors
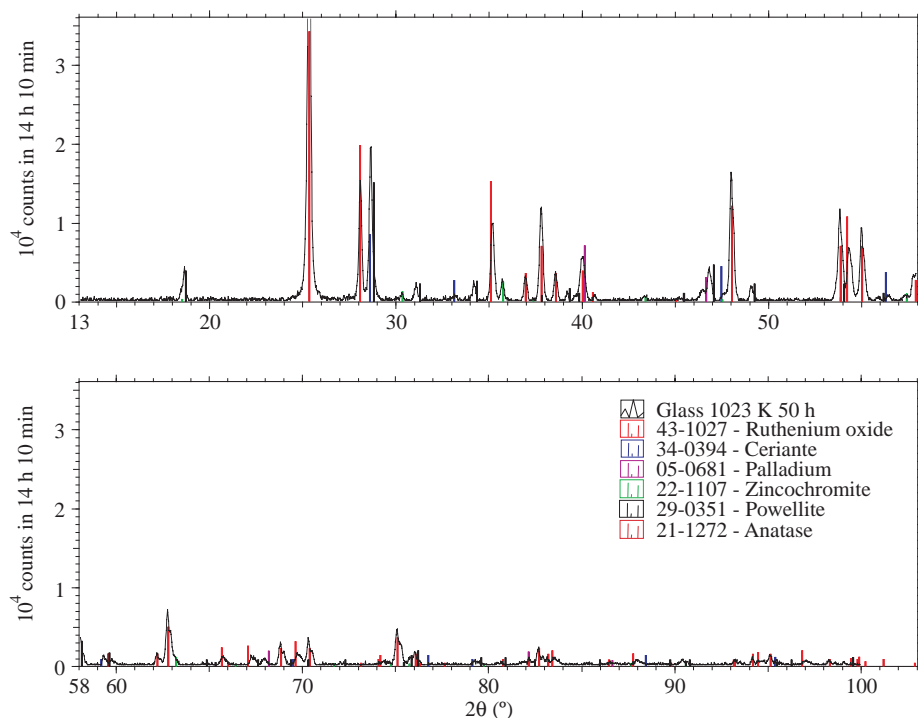
**Figure 1**
Background-subtracted X-ray diffraction diagram for glass heat-treated for 50 h at 1023 K, containing the internal standard (TiO$_2$): identification of crystalline phases.

10 mm$^2$) in order to determine the area fraction of each phase with good accuracy. The area fractions were then converted to weight fractions using the phase densities. The comparison of results (Table 4) is valid only for platinoid elements because they were present in the quenched glass and are unaffected by the heat treatment. The results show a satisfactory correlation for the RuO$_2$ phase. The low value obtained by image analysis resulted from the low optical contrast between the crystalline phase and the glass. For the Pd–Te solid-solution percentages, more significant discrepancies were observed between the Rietveld method and the others. This can be attributed not only to the size distribution of the spherical Pd–Te particles (1–25 µm radius in opposition to the constant-size assumption), but also to the possible existence and/or dissolution of uncrystallized palladium in the glass. Moreover, the X-ray diffraction analysis was performed on small (0.5 g) glass fragments, whereas the high density of the platinoid elements and the stirring action during glass preparation favoured an inhomogeneous particle distribution.

appear to arise more from a lack of homogeneity in the powder and from the choice of the internal standard (overlap, intensity).

In order to validate the quantitative results obtained by applying the Rietveld method, X-ray fluorescence chemical analysis and optical microscopic analysis were also performed. The optical micrographs were examined using an automatic image analyser. The analysis was carried out to 100 fields (*i.e.*

### 4.4. Refinement of the site occupancy

The classical method for assessing the composition of the crystalline structure consists of direct refinement of the site occupancy, a parameter specific to each element in the unit cell, corresponding to the extent of occupation by each element and indicating the occurrence of possible substitutions. It is refined in parallel with the positional parameters. The substitution of one element by another can thus be detected by X-ray diffraction only when the elements are relatively distant in the Periodic Table.

Refinement of the calcium occupancy in the CaMoO$_4$ phase showed an increase in the occupancy (which exceeded 100%), indicating substitution of calcium by elements of higher atomic weight. The heavy elements substituted in octahedral coordination in the CaMoO$_4$ crystal were identified by elemental electron microprobe analysis. The results (Table 5) confirmed the presence of
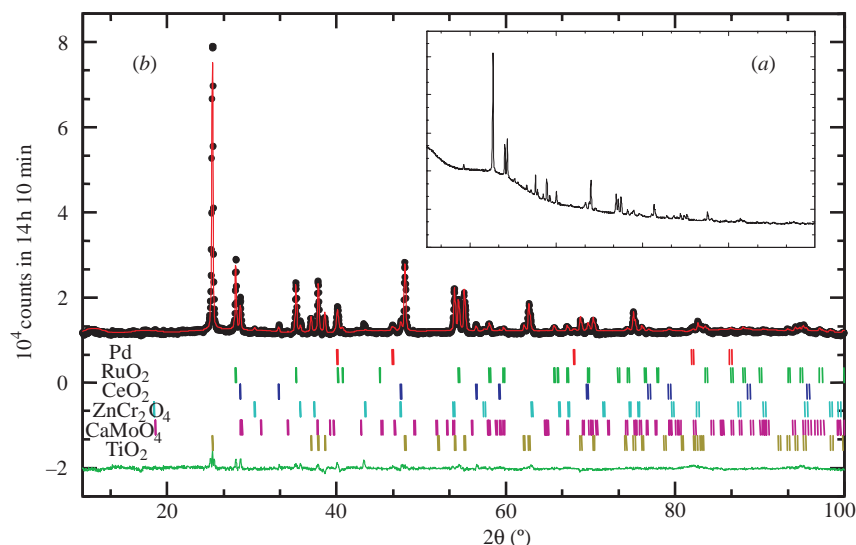


**Figure 2**
(*a*) X-ray diffraction diagram for glass heat-treated for 50 h at 1023 K, containing the internal standard (TiO$_2$); (*b*) Rietveld refinement of the diffraction profiles after elimination of the continuous background. Comparison of the observed (black) and calculated (red) diagrams with the difference diagram (green).

**Table 3**
Linear absorption coefficients $\mu_{\varphi}$ and values corrected for the presence of the internal standard $(W_{\varphi})_{raw}$ (wt%) before microabsorption correction (BMC) and after microabsorption correction (AMC) applying the Brindley method.

| Phase | $\mu_{\varphi}$ (cm$^{-1}$) | $(W_{\varphi})_{raw}$ quenched glass | | $(W_{\varphi})_{raw}$ after heat treatment at 1023 K | | | | | |
| | | | | 20 h | | 50 h | | 1000 h | |
| | | BMC | AMC | BMC | AMC | BMC | AMC | BMC | AMC |
|---|---|---|---|---|---|---|---|---|---|
| RuO$_2$ | 350 | 1.66 | 1.69 (10) | 1.57 | 1.97 (11) | 0.90 | 1.09 (10) | 1.18 | 1.48 (10) |
| Pd–Te | 215 | 0.27 | 0.27 (10) | 0.37 | 0.39 (10) | 0.22 | 0.22 (10) | 0.23 | 0.23 (6) |
| CaMoO$_4$ | 195 | – | – | 1.47 | 1.50 (25) | 1.56 | 1.63 (10) | 1.87 | 1.92 (26) |
| CeO$_2$ | 733 | – | – | 0.04 | 0.06 (7) | 0.08 | 0.11 (3) | 0.41 | 0.60 (8) |
| ZnCr$_2$O$_4$ | 254 | – | – | 0.09 | 0.10 (13) | 0.19 | 0.19 (5) | 0.70 | 0.78 (14) |
| Amorphous | 110 | – | 98.04 (20) | – | 95.98 (66) | – | 96.76 (38) | – | 94.99 (64) |

**Table 4**
Platinoid weight percentages measured by the Rietveld method and by chemical and optical analyses.

| Crystalline phase | Theoretical percentage in the glass (wt%) | Mean $(W_{\varphi})_{raw}$ (wt%) | Chemical analysis (wt%) | Optical analysis (converted in wt%) |
|---|---|---|---|---|
| RuO$_2$ | 1.58 | 1.56 (20) | 1.49 (22) | 1.27 (40) |
| Pd–Te | 1.20 | 0.28 (20) | 0.90 (14) | 0.93 (20) |

**Table 5**
Elemental analysis of calcium molybdate by electron microprobe.

| | Ca | Mo | Sr | La | Nd | Na | O |
|---|---|---|---|---|---|---|---|
| Possible coordination numbers (Shannon & Prewitt, 1969) | $\geq 6$ | 4 | $\geq 6$ | $\geq 6$ | $\geq 6$ | $\geq 4$ | |
| Theoretical composition (wt%) | 20.05 | 47.96 | – | – | – | – | 31.99 |
| Experimental composition (wt%) | 14.73 (21) | 45.29 (92) | 1.62 (10) | 1.23 (9) | 2.41 (17) | 1.34 (13) | 33.38 (75) |

strontium, lanthanum and neodymium within the crystal. The natural coordination number of these three compounds also suggests that they substituted calcium. Note that oxygen composition was deduced by subtracting the sum of the element compositions. The experimental composition 12.2Ca–15.6Mo–0.6Sr–0.3La–0.6Nd–1.9Na–68.8O (at.%) gives reasonable charge balance.

## 5. Conclusions

This study demonstrates the possibility of using the Rietveld method to determine the weight percentages of several crystalline phases within a predominantly (>95 wt%) amorphous material. The corrections for microabsorption effects resulted in higher percentages for the crystalline components. Despite the small crystallized fractions, site-occupancy refinement revealed the existence of substitutions for Ca within the CaMoO$_4$ structure and refinement of the unit-cell parameters provided information on the composition of the Pd–Te solid solution. These results were confirmed by electron microprobe chemical analysis. Systematic application of this method to glass samples submitted to various heat-treatment scenarios will be used to plot time–temperature–transformation (TTT) diagrams that will indicate the cooling rates applicable to obtain vitreous or glass ceramic materials.

## References

Bish, D. L. & Howard, S. A. (1988). *J. Appl. Cryst.* **21**, 86–91.
Brindley, G. W. (1945). *Philos. Mag.* **36**, 347–369.
Chattopadhyay, G., Bhatt, Y. J. & Khera, S. K. (1986). *J. Less-Common Met.* **123**, 251–266.
*International Tables for Crystallography* (1983). Vol. *A*. Dordrecht: D. Reidel.
Orlhac, X., Fillet, C. & Phalippou, J. (1998). *Scientific Basis for Nuclear Waste Management XXII (Boston, USA), Material Research Symposium Proceedings*, Vol. 556. In the press.
Rietveld, H. M. (1969). *J. Appl. Cryst.* **2**, 65–71.
Rodriguez-Carvajal, J. (1993). *Physica B*, **192**, 55–69.
Shannon, R. D. & Prewitt, C. T. (1969). *Acta Cryst.* B**25**, 925–946.
Yasukawa, K., Terashi, Y. & Nakayama, A. (1998). *J. Am. Ceram. Soc.* **81**, 2978–2982.